



SCIENCE AND TECHNOLOGY ORGANIZATION  
CENTRE FOR MARITIME RESEARCH AND EXPERIMENTATION



**Reprint Series**

**CMRE-PR-2019-035**

# **Prediction of rendezvous in maritime situational awareness**

Murat Uney, Leonardo M. Millefiori, Paolo Braca

May 2019

Originally published in:

Proc. of the 21st International Conference on Information Fusion (FUSION 2018),  
Cambridge 2018, pp. 622-628, doi: [10.23919/ICIF.2018.8455816](https://doi.org/10.23919/ICIF.2018.8455816)

## About CMRE

The Centre for Maritime Research and Experimentation (CMRE) is a world-class NATO scientific research and experimentation facility located in La Spezia, Italy.

The CMRE was established by the North Atlantic Council on 1 July 2012 as part of the NATO Science & Technology Organization. The CMRE and its predecessors have served NATO for over 50 years as the SACLANT Anti-Submarine Warfare Centre, SACLANT Undersea Research Centre, NATO Undersea Research Centre (NURC) and now as part of the Science & Technology Organization.

CMRE conducts state-of-the-art scientific research and experimentation ranging from concept development to prototype demonstration in an operational environment and has produced leaders in ocean science, modelling and simulation, acoustics and other disciplines, as well as producing critical results and understanding that have been built into the operational concepts of NATO and the nations.

CMRE conducts hands-on scientific and engineering research for the direct benefit of its NATO Customers. It operates two research vessels that enable science and technology solutions to be explored and exploited at sea. The largest of these vessels, the NRV Alliance, is a global class vessel that is acoustically extremely quiet.

CMRE is a leading example of enabling nations to work more effectively and efficiently together by prioritizing national needs, focusing on research and technology challenges, both in and out of the maritime environment, through the collective Power of its world-class scientists, engineers, and specialized laboratories in collaboration with the many partners in and out of the scientific domain.



**Copyright © IEEE, 2018.** NATO member nations have unlimited rights to use, modify, reproduce, release, perform, display or disclose these materials, and to authorize others to do so for government purposes. Any reproductions marked with this legend must also reproduce these markings. All other rights and uses except those permitted by copyright law are reserved by the copyright owner.

**NOTE:** The CMRE Reprint series reprints papers and articles published by CMRE authors in the open literature as an effort to widely disseminate CMRE products. Users are encouraged to cite the original article where possible.

---

# Prediction of Rendezvous in Maritime Situational Awareness

Murat Üney, Leonardo M. Millefiori, Paolo Braca

NATO Science & Technology Organisation

Centre for Maritime Research and Experimentation

Viale San Bartolomeo 400, 19126 La Spezia SP, Italy

{ murat.oney, leonardo.millefiori, paolo.braca } @ nato.cmre.int

**Abstract**—In this work, we consider the problem of algorithmically predicting rendezvous among vessels based on their trajectory forecasts in a maritime environment. The problem is treated as hypothesis testing on the expected value of the distance between trajectories. We relate this quantity to the first and second degree Wasserstein distances between trajectory forecast distributions. These distributions are obtained using integrated Ornstein-Uhlenbeck process models with the trajectory measurements collected so far. Building upon these results, we propose an algorithm which traverses the trajectories observed so far for detecting rendezvous over a rolling time horizon. We demonstrate the efficacy of the proposed algorithm using simulations.

**Index Terms**—predictive models, knowledge discovery, mean reverting process, Integrated Ornstein-Uhlenbeck process, Wasserstein distance, situation awareness

## I. INTRODUCTION

This work considers the problem of deciding on whether two vessels are likely to engage at a future time instant based on their currently observed trajectories, i.e., prediction of rendezvous. The capability of algorithmically carrying out this task is extremely valuable in maritime surveillance applications given that the high levels of uncertainty in the environment together with the abundance of traffic data, e.g., automatic identification system (AIS) messages, make it extremely difficult for human operators to perform with the desired accuracy in a robust and sustainable fashion [1].

We treat the problem as hypothesis testing over a rolling time horizon which involves forecasting of future state trajectories in terms of probability densities over state variables. In particular, the expected distance between two vessels is considered as the decision statistics. It is not straightforward to evaluate this quantity, in general. Instead, we relate it to the Wasserstein distances [2] of individual trajectory forecast distributions. These distributions are obtained by using integrated Ornstein-Uhlenbeck (OU) process trajectory models [3]. Specifically, we point out that the Wasserstein distance of the second degree between the forecast distributions upper bound the expected distance of concern. Moreover, this distance can be computed easily for multi-variate Gaussian

distributions [4] which is the case when OU models are used for trajectory forecasting.

Based upon these results, we propose an algorithm that traverses the trajectory data over time and searches for pairs of forecast distributions with a Wasserstein distance of the second degree below a selected distance. Equivalently, pairs with an expected distance upper bounded below a given threshold are found.

Algorithmic knowledge discovery based on predictive models of trajectories has an increasing relevance to situation awareness applications and autonomous systems. In maritime situation awareness, this is facilitated by the AIS in which ships asynchronously broadcast messages that contain their identity, position, velocity and some other vessel/voyage related information. AIS data have been used for finding recurrent or regular patterns of vessel trajectories as well as anomalies (see, e.g., [1], [5]) and modelling maritime traffic [6]. In these applications, OU process models have proved useful [3]. In autonomous system applications, intent prediction is posed as an  $M$ -ary hypothesis testing problem on trajectories modelled using bridging densities [7]. Our problem differs in that a rendezvous hypothesis involve a dynamic intention for the engaging parties. Bayesian inference in stochastic processes with directed interactions have been investigated in [8]. The problem setting in this work is related long-term forecasting in which case these interactions involve a very high degree of uncertainty and an undirected nature. This further motivates the use of our geometric perspective and the Wasserstein distance as the computation of the latter accounts for a certain extent of interactions. This point is clarified throughout the article.

The structure of this article is as follows: The rendezvous hypothesis and a conceptual search algorithm are introduced in Section II. Section III introduces the Wasserstein distance between forecast distributions and relates it to the decision statistics of the conceptual search. Then, we provide explicit formulae for the forecast distributions in Section IV. In Section V, we propose a computationally feasible search Algorithm for rendezvous detection based on the second degree Wasserstein distance of these distributions. In Section VI, we demonstrate the efficacy of this algorithm through a simulation example. Then, we conclude in Section VII.

This work is supported by the NATO Allied Command Transformation (ACT) via the project Data Knowledge Operational Effectiveness (DKOE) at the NATO Science and Technology Organization (STO) Centre for Maritime Research and Experimentation (CMRE).

## II. PROBLEM STATEMENT

Let us consider  $N$  trajectories  $\mathcal{H} = \{h^i | i = 1, \dots, N\}$  each consisting of a series of time and state pairs

$$h^i \triangleq \{(t_k^i, x_k^i) | k = 1, \dots, K^i\} \quad (1)$$

where the state variable  $x_k^i$  is a concatenation of the location and velocity of the  $i^{th}$  object, i.e.,  $x_k^i = [s_k^i, \dot{s}_k^i]$  where  $s_k^i$  is the location variable that takes values from a bounded set  $\mathfrak{S} \subseteq \mathbb{R}^2$  and the velocity variable  $\dot{s}_k^i \in \mathfrak{V} \subseteq \mathbb{R}^2$ . These pairs are assumed to be noise-free measurements, and, in a maritime scenario, correspond to AIS messages from the vessels<sup>1</sup>. Thus, at current time  $t_s$ , the time stamps of the trajectories satisfy

$$t_s \geq \max\{t_{K^i}^i : i = 1, \dots, N\},$$

and, we denote the available trajectories at time  $t_s$  by  $\mathcal{H}_{t_s}$  throughout.

Stochastic process models [9], [10] for these trajectories induce a (conditional) probability distribution over the concatenation of object states at an arbitrary time  $t$ . Let us denote this random variable by  $\mathbf{X}_t$ . Thus, a realisation  $X_t = [x_t^1, \dots, x_t^N]$  of this random variable is distributed by  $P_t(\cdot | \mathcal{H}_{t_s})$  satisfying

$$Pr\{X_t \in \mathcal{S}\} = \int_{\mathcal{S}} dP_t(X_t | \mathcal{H}_{t_s}), \quad (2)$$

where  $\mathcal{S} \subset \mathfrak{S} \times \mathfrak{V}$ . Let us also assume that this distribution has a density  $p_t(X_t | \mathcal{H}_{t_s})$  allowing us to compute (2) through

$$Pr\{X_t \in \mathcal{S}\} = \int_{\mathcal{S}} p_t(X_t | \mathcal{H}_{t_s}) dX_t. \quad (3)$$

We are concerned with the hypothesis that two vessels  $(i, j)$  have a rendezvous at time  $t^r \in T$  where  $T = [t_s, t_f]$  is a rolling horizon time window of length  $t_f - t_s = \Delta T$ . In other words, we are concerned with the distance process, a realisation of which is given by

$$d^{i,j}(t^r) = \left\| s_{t^r}^i - s_{t^r}^j \right\| \quad (4)$$

for  $t^r \in T$ , where  $s_{t^r}^i$  and  $s_{t^r}^j$  are realisations of the random (location) variables of the state at  $t^r$  and are characterised by the marginal of the density in (3) over  $(s^i, s^j)$ , i.e.,  $p_{t^r}^{i,j}(s_{t^r}^i, s_{t^r}^j | \mathcal{H}_{t_s})$ , and,  $\|\cdot\|$  denotes the  $l_2$  norm.

Let us consider the first order statistical moment of  $d^{i,j}(t^r)$ , i.e., the expected value of the random variable  $\mathbf{d}^{i,j}(t^r)$

$$E\{\mathbf{d}^{i,j}(t^r)\} = \int_{\mathfrak{S} \times \mathfrak{S}} \left\| s_{t^r}^i - s_{t^r}^j \right\| p_{t^r}^{i,j}(s_{t^r}^i, s_{t^r}^j | \mathcal{H}_{t_s}) ds_{t^r}^i ds_{t^r}^j. \quad (5)$$

Using this quantity, one decides on the rendezvous hypothesis  $R_{t^r}^{i,j}$  for the pair  $(i, j)$  by

$$E\{\mathbf{d}^{i,j}(t^r)\} \underset{R_{t^r}^{i,j}=0}{\overset{R_{t^r}^{i,j}=1}{\gtrless}} \gamma, \quad (6)$$

<sup>1</sup>The inaccuracies in the state observations reported in AIS messages are negligible compared to the uncertainties captured in forecast distributions that are introduced later. This fact underlies the assumption that the observations are noise free. The trajectory forecasting process detailed later in the article can easily accommodate for such uncertainties if necessary.

where  $\gamma$  is a decision threshold of the same unit as the  $l_2$  norm, i.e., meters.

The stochastic model specifies a metric valued decision variable for the problem which allows us to select a tangible decision threshold. Because the associated rendezvous event is parameterised on time, a search is implied over the space that these variables take values from in order find the rendezvous.

A conceptual temporal search building upon the stochastic model above is given by Algorithm 1. For all trajectory pairs  $(i, j)$ , location predictions are found at each time instant  $t^r \in T$  by first finding the density in (3) and marginalising out all variables other than  $(s_{t^r}^i, s_{t^r}^j)$  (line 8). This forecast is used to find the expected distance in (5) (line 9). Those time points with an expectation below the decision threshold are added to the list of rendezvous events to be pruned later by the selection of the soonest rendezvous decision for  $(i, j)$ . The minimum mean squared error prediction of the vessel locations are used to predict to rendezvous point. Hence, this search returns a list of rendezvous  $\mathcal{R}$  reporting (at most) a single detection per pair together with its time and location.

There is a number of challenges in realising Algorithm 1 which are addressed in the rest of this article. First, it is not trivial to find a tractable form for the prediction density in (3) (line 8), especially, in the presence of (unknown) interactions among the vessels. This also complicates the evaluation of (5) in line 9. In Section III, we relate the expected distance to the Wasserstein distance of the first degree and then detail computation of the forecasting densities individual trajectories in Section IV. Section V builds upon these results and specifies a rendezvous detection algorithm that uses an explicit formulae for the second degree Wasserstein distance of the trajectory forecasts upper bounding the distance expectation. Last but

---

**Algorithm 1** A conceptual temporal search for rendezvous prediction.

---

- 1: Input:  $\mathcal{H}$  ▷ Current trajectory data in (1)
  - 2: Input:  $\gamma$  ▷ Decision threshold in meters
  - 3: Input:  $T$  ▷ Temporal search space
  - 4:  $\mathcal{R} \leftarrow \emptyset$
  - 5: **for all**  $i = 1, \dots, N, j = i + 1, \dots, N$  **do**
  - 6:    $\mathcal{R}^{i,j} \leftarrow \emptyset$
  - 7:   **for all**  $t^r \in T$  **do**
  - 8:     Find  $p_{t^r}^{i,j}(s_{t^r}^i, s_{t^r}^j | \mathcal{H}_{t_s})$  ▷ Forecasting  $i$  and  $j$
  - 9:      $\hat{d}^{i,j}(t^r) \leftarrow E\{\mathbf{d}^{i,j}(t^r)\}$  ▷ Evaluate (5)
  - 10:     **if**  $\hat{d}^{i,j}(t^r) \leq \gamma$  **then** ▷ Decision test
  - 11:        $(\hat{s}_{t^r}^i, \hat{s}_{t^r}^j) \leftarrow E\{s_{t^r}^i, s_{t^r}^j | \mathcal{H}_{t_s}\}$  ▷ State prediction
  - 12:        $\hat{s}^r = (\hat{s}_{t^r}^i + \hat{s}_{t^r}^j)/2$  ▷ Rendezvous point prediction
  - 13:        $\mathcal{R}^{i,j} \leftarrow \mathcal{R}^{i,j} \cup \{(t^r, \hat{s}^r)\}$
  - 14:     **end if**
  - 15:   **end for**
  - 16:    $t^* = \arg \min_{t^r \in \mathcal{R}^{i,j}} \{t^r\}, s^* = \mathcal{R}^{i,j}(t^*)$
  - 17:    $\mathcal{R} \leftarrow \mathcal{R} \cup \{(i, j, t^*, s^*, \hat{d}^{i,j}(t^*))\}$
  - 18: **end for**
  - 19: **Return**  $\mathcal{R}$
-

not least, the temporal search space is continuous which, in practice, needs to be discretised, e.g., by forming a uniform grid over  $T$ .

### III. WASSERSTEIN DISTANCE OF THE FIRST DEGREE AS THE DISTANCE EXPECTATION

Let us consider the decision variable in (6) which is an expectation with the underlying distribution specified by a marginal of the joint forecast distribution. Furthermore, this distribution is conditioned on the entire set of trajectory measurements  $\mathcal{H}_{t_s} = \{h_{t_s}^i | i = 1, \dots, N\}$  at the current time  $t_s$ . As a result, this density embodies all interactions of  $(i, j)$  – with other vessels and mutual – up until the current time. There is a high level of uncertainty on the type and strength of these interactions and exact inference on these does not scale well with  $N$ , on the other hand (see, e.g., [8] for inference in social force models and the discussion on the complexity of inference). This is exacerbated by the uncertainty on how future interactions are related to currently existing ones. Therefore, it is reasonable to invoke the assumption that the future forecasts are independent from the interactions until  $t_s$ , i.e.,

$$p_{t_r}^i(s_{t_r}^i | \mathcal{H}_{t_s}) = p_{t_r}^i(s_{t_r}^i | h_{t_s}^i) \quad (7)$$

for all  $i = 1, \dots, N$ , where the left hand side of the equality is the  $i$ th marginal of the joint forecast density given all observations, and, the right hand side is the individual forecast for  $i$  based on only its own trajectory's observations until now.

Future interactions, on the other hand, are assumed to take any form for pairs of vessels with the constraint that their joint forecast density has marginals as given in (7). Let us denote the set of such densities by  $\mathcal{P}^{i,j}$ . Thus, the expected distance in (6) is related to the Wasserstein distance of the first degree [2] between the distributions  $P_i, P_j$  associated respectively with the densities  $p_{t_r}^i(s_{t_r}^i | h_{t_s}^i)$  and  $p_{t_r}^j(s_{t_r}^j | h_{t_s}^j)$  as follows:

$$\begin{aligned} W_1(P_i, P_j) &\triangleq \inf_{p \in \mathcal{P}^{i,j}} \int \left\| s_{t_r}^i - s_{t_r}^j \right\| p(s_{t_r}^i, s_{t_r}^j | h_{t_s}^i, h_{t_s}^j) ds_{t_r}^i ds_{t_r}^j, \\ &= \inf_{p \in \mathcal{P}^{i,j}} E_p \{ \mathbf{d}_{t_r}^{i,j} \}. \end{aligned} \quad (8)$$

Note that, 1-Wasserstein distance gives the minimum distance that vessels  $i, j$  are expected to approach each other by accounting for any form of interaction that leads to a joint forecast distribution with marginals specified in (7). This result motivates the following modifications in Algorithm 1: i) The replacement of the forecast density in line 8 with the individual densities for  $i$  and  $j$  as given in (7), ii) the replacement of the decision statistics in line 9 with  $W_1(P_i, P_j)$  in (8).

The computation of  $W_1$ , on the other hand, involves solving an optimisation problem which should not be expected to have a straightforward solution for general distributions. In the next section, we detail how the individual forecast distributions are found. Then, in Section V, we introduce the Wasserstein distance of degree 2 as an upper bound to  $W_1$  that is feasible to compute building upon the results in the next section.

### IV. FINDING INDIVIDUAL FORECAST DISTRIBUTIONS: LONG-TERM TRAJECTORY PREDICTION USING OU PROCESS MODELS

Let us consider  $p_{t_r}^i(x_{t_r}^i | h_{t_s}^i)$  where  $t_r$  is a future time that we are interested in predicting the state  $x_{t_r}^i = [s_{t_r}^i, \dot{s}_{t_r}^i]$  of vessel  $i$  for given all of its trajectory samples up to time  $t_s$  denoted by  $h_{t_s}^i$ . This density and its distribution are specified by the stochastic process which generates the (continuous) state trajectory  $x_t^i$  over time. For the sake of brevity in exposition, let us slightly modify the notation in this section and denote this density by  $p(\mathbf{x}[K+1] | \mathbf{x}[K], \dots, \mathbf{x}[1])$ , where we dropped the superscript  $i$ , and, used  $\mathbf{x}[K+1]$  to denote  $x_{t_r}^i$ , and,  $\mathbf{x}[K], \dots, \mathbf{x}[1]$  to capture the trajectory samples in  $h_{t_s}^i$ .

OU processes have recently proved useful in capturing the characteristics of vessel trajectories in the maritime domain [3]. The remarkable feature of this model is that the velocity component tends to a (latent) mean value with an attraction proportional to the deviation from the mean. Thus, the variance of the velocity component remains bounded, and, its mean successfully captures the desired cruise velocity of the ship. The state dynamics of this model is described by

$$\dot{\mathbf{x}}(t) = \begin{bmatrix} \mathbf{0}, & \mathbf{I} \\ \mathbf{0}, & -\mathbf{\Gamma} \end{bmatrix} \mathbf{x}(t) + \begin{bmatrix} \mathbf{0} \\ \mathbf{\Gamma} \end{bmatrix} \mathbf{v} + \begin{bmatrix} \mathbf{0} \\ \mathbf{H} \end{bmatrix} \dot{\mathbf{n}}(t), \quad (9)$$

where  $\mathbf{0}$  and  $\mathbf{I}$  are the  $2 \times 2$  null and identity matrices, respectively. Here,  $\mathbf{n}(t)$  is a 2-D Wiener process, and,  $\mathbf{v} = [v_x, v_y]^T$  is the aforementioned mean velocity parameter. The mean reverting behaviour is controlled by the square matrix  $\mathbf{\Gamma} \in \mathbb{R}^{2 \times 2}$  which is the second latent parameter of the process. The third parameter  $\mathbf{H}$  effectively specifies the *process* noise covariance which will be clarified later in this section.

In order to find the relevant distributions of the state random variables induced by the dynamics in (9), we discretise this equation. The stochastic differential equation sampled at  $t_1, \dots, t_K, t_{K+1}$  is a difference equation given by

$$\mathbf{x}[k] = \mathbf{\Phi}(\Delta t_k, \mathbf{\Gamma}) \mathbf{x}[k-1] + \mathbf{\Psi}(\Delta t_k, \mathbf{\Gamma}) \mathbf{v} + \mathbf{n}_k \quad (10)$$

for  $k = 2, \dots, K+1$  where  $\mathbf{n}_k$  is a Gaussian variable with zero mean and  $\mathbf{\Sigma}_n$  covariance<sup>2</sup>. The state transition and input forcing matrices  $\mathbf{\Phi}$  and  $\mathbf{\Psi}$  here represent linear transforms which are specified by the time difference  $\Delta t_k \triangleq t_k - t_{k-1}$ , and, the transform  $\mathbf{\Gamma}$ .

At this point, it is worthwhile to notice that the above difference equation indicates that the probability density  $p(\mathbf{x}[K+1] | \mathbf{x}[K], \dots, \mathbf{x}[1], \mathbf{v}, \mathbf{\Gamma}, \mathbf{H})$  is first-order Markov in  $\mathbf{x}[k]$ s, i.e.,

$$p(\mathbf{x}[k] | \mathbf{x}[k-1], \dots, \mathbf{x}[1], \mathbf{v}, \mathbf{\Gamma}, \mathbf{H}) = p(\mathbf{x}[k] | \mathbf{x}[k-1], \mathbf{v}, \mathbf{\Gamma}, \mathbf{H}). \quad (11)$$

<sup>2</sup>Here, the covariance  $\mathbf{\Sigma}_n$  is related to  $\mathbf{H}$  in (9) which specifies the power spectral density of the Wiener process, the time difference  $t_k - t_{k-1}$ , and,  $\mathbf{\Gamma}$ . The structure of this matrix is given later in this Section. Further details can be found in Appendix A in [3]. For the purposes of this article, it suffices to assume that  $\mathbf{\Sigma}_n$  is a regular covariance matrix that is positive definite and symmetric after the discretisation.

Furthermore, this density is Gaussian with a covariance of  $\Sigma_n$ , and, a mean vector given by the first two terms on the right hand side of (10) , i.e.,

$$p(\mathbf{x}[k]|\mathbf{x}[k-1], \mathbf{v}, \mathbf{\Gamma}, \mathbf{H}) = \mathcal{N}(\mathbf{x}[k]; \mathbf{\Phi}(\Delta t_k, \mathbf{\Gamma})\mathbf{x}[k-1] + \mathbf{\Psi}(\Delta t_k, \mathbf{\Gamma})\mathbf{v}, \Sigma_n). \quad (12)$$

On the other hand,  $\mathbf{v}, \mathbf{\Gamma}$  and  $\mathbf{H}$  are typically unknown and differ for each vessel  $i$ . Therefore, the Markov property above is not valid for the forecast distribution of concern: The density seeked is found by using the chain rule of probabilities and marginalising out these parameters:

$$p(\mathbf{x}[k]|\mathbf{x}[k-1], \dots, \mathbf{x}[1]) = \int p(\mathbf{x}[k]|\mathbf{x}[k-1], \mathbf{v}, \mathbf{\Gamma}, \mathbf{H}) \times p(\mathbf{v}, \mathbf{\Gamma}, \mathbf{H}|\mathbf{x}[k-1], \dots, \mathbf{x}[1]) d\mathbf{v} d\mathbf{\Gamma} d\mathbf{H}. \quad (13)$$

This integration is not straightforward to perform, however. Selection of (non-informative) priors in order to find the parameter posterior inside the marginalisation is similarly non-trivial. In this work, we instead use an empirical Bayes approach [11], and, approximate the integration in (13) by first finding the maximum likelihood estimates of  $\mathbf{v}, \mathbf{\Gamma}$  and  $\mathbf{H}$ . Then, these quantities are substituted in (11)–(12), i.e.,

$$p(\mathbf{x}[k]|\mathbf{x}[k-1], \dots, \mathbf{x}[1]) \approx p(\mathbf{x}[k]|\mathbf{x}[k-1], \hat{\mathbf{v}}_{ML}, \hat{\mathbf{\Gamma}}_{ML}, \hat{\mathbf{H}}_{ML}), \quad (14)$$

where

$$(\hat{\mathbf{v}}_{ML}, \hat{\mathbf{\Gamma}}_{ML}, \hat{\mathbf{H}}_{ML}) = \arg \max_{\mathbf{v}, \mathbf{\Gamma}, \mathbf{H}} l(\mathbf{x}[k-1], \dots, \mathbf{x}[1]|\mathbf{v}, \mathbf{\Gamma}, \mathbf{H}). \quad (15)$$

Note that the quality of this approximation improves as the number of data samples increases. Details of the ML estimators can be found in [3]. Let us now give explicit formulae for  $\mathbf{\Phi}, \mathbf{\Psi}$ , and,  $\Sigma_n$  in order to specify the mean and covariance in (12). First, let us consider a positive definite  $\mathbf{\Gamma}$  such that

$$\mathbf{\Gamma} = \mathbf{E}\mathbf{\Theta}\mathbf{E}^T, \quad \mathbf{\Theta} = \begin{bmatrix} \gamma_1 & 0 \\ 0, & \gamma_2 \end{bmatrix} \quad (16)$$

where  $\mathbf{E}$  is a unitary matrix with eigenvectors of  $\mathbf{\Gamma}$  at its coloumns, and,  $T$  denotes matrix transpose. Then, the following equalities hold [3]:

$$\mathbf{\Phi}(\Delta t, \mathbf{\Gamma}) = \tilde{\mathbf{E}} \begin{bmatrix} \mathbf{I}, & (\mathbf{I} - \exp(-\mathbf{\Gamma}\Delta t) \mathbf{\Gamma}^{-1}) \\ \mathbf{0}, & \exp(-\mathbf{\Gamma}\Delta t) \end{bmatrix} \tilde{\mathbf{E}}^T, \\ \mathbf{\Psi}(\Delta t, \mathbf{\Gamma}) = \tilde{\mathbf{E}} \begin{bmatrix} \Delta t \mathbf{I} - (\mathbf{I} - \exp(-\mathbf{\Gamma}\Delta t) \mathbf{\Gamma}^{-1}) \\ \mathbf{I} - \exp(-\mathbf{\Gamma}\Delta t) \end{bmatrix} \tilde{\mathbf{E}}^T$$

where  $\tilde{\mathbf{E}} = \mathbf{I} \otimes \mathbf{E}$  with  $\otimes$  denoting the Kronecker product. The covariance of concern is given by

$$\Sigma_n = \tilde{\mathbf{E}} \Sigma_1 \circ \Sigma_2(\Delta t) \tilde{\mathbf{E}}^T \quad (17)$$

where  $\circ$  denotes the Hadamard product of the two matrices  $\Sigma_1$  and  $\Sigma_2(\Delta t)$  defined in [3, Eq.s (41),(52)–(55)].

Finally, note that  $p_{tr}^i(s_{tr}^i|h_{ts}^i)$  on the right hand side of (7)

is obtained by marginalising the state prediction density over the velocity variable, i.e.

$$p_{tr}^i(s_{tr}^i|h_{ts}^i) = \int_{\mathfrak{D}} p_{tr}^i(x_k^i|h_{ts}^i) ds_k^i. \quad (18)$$

This density can explicitly be found as a Gaussian of the form  $\mathcal{N}(s_{tr}^i; \mu^i, \Sigma^i)$  by using marginalisation rules on multi-variate Gaussians with (12)–(15).

## V. RENDEZVOUS DETECTION USING THE WASSERSTEIN DISTANCE OF THE SECOND DEGREE

The 2-Wasserstein distance of the individual forecast distributions over  $\mathbb{R}^2$  induced by the  $l_2$  norm is given by [2]

$$W_2(P_i, P_j) \triangleq \inf_{p \in \mathcal{P}^{i,j}} \int \|s^i - s^j\|^2 p(s_{tr}^i, s_{tr}^j|h_{ts}^i, h_{ts}^j) ds_{tr}^i ds_{tr}^j)^{1/2}. \quad (19)$$

This quantity upper bounds their 1-Wasserstein distance introduced in Section III [2], i.e.,

$$E\{\mathbf{d}_{tr}^{i,j}\} = W_1(P_i, P_j) \leq W_2(P_i, P_j), \quad (20)$$

and, can be found in closed form for multi-variate Gaussians. Specifically, for  $p(s^i|h^i; t^r) = \mathcal{N}(s^i; \mu^i, \Sigma^i)$  and

---

**Algorithm 2** Rendezvous prediction using the 2-Wasserstein distance of prediction distributions.

---

- 1: Input:  $\mathcal{H}$  ▷ Current trajectory data in (1)
  - 2: Input:  $\gamma$  ▷ Decision threshold in meters
  - 3: Input:  $T$  ▷ Temporal search space
  - 4:  $\mathcal{R} \leftarrow \emptyset$
  - 5: **for all**  $i = 1, \dots, N$  **do**
  - 6:   **for all**  $t^r \in T$  **do**
  - 7:     Find  $\mathcal{N}(s_{tr}^i; \mu^i, \Sigma^i)$  ▷ Forecasting (see Section IV)
  - 8:   **end for**
  - 9: **end for**
  - 10: **for all**  $i = 1, \dots, N, j = i + 1, \dots, N$  **do**
  - 11:    $\mathcal{W}^{i,j} \leftarrow \emptyset$
  - 12:   **for all**  $t^r \in T$  **do**
  - 13:      $W_{i,j}(t^r) \leftarrow W_2(P_i, P_j)$  ▷ Find the 2-Wasserstein distance in (21)
  - 14:     **if**  $W_{i,j}(t^r) \leq \gamma$  **then** ▷ Decision test
  - 15:        $\hat{s}_{tr}^i \leftarrow \mu^i$  ▷ State prediction for  $i$
  - 16:        $\hat{s}_{tr}^j \leftarrow \mu^j$  ▷ State prediction for  $j$
  - 17:        $\hat{s}^r = (\hat{s}_{tr}^i + \hat{s}_{tr}^j)/2$  ▷ Rendezvous point prediction
  - 18:        $\mathcal{R}^{i,j} \leftarrow \mathcal{R}^{i,j} \cup \{(t^r, \hat{s}^r)\}$
  - 19:     **end if**
  - 20:   **end for**
  - 21:    $t^* = \arg \min_{t^r \in \mathcal{R}^{i,j}} \{t^r\}, s^* = \mathcal{R}^{i,j}(t^*)$
  - 22:    $\mathcal{R} \leftarrow \mathcal{R} \cup \{(i, j, t^*, s^*, \hat{d}^{i,j}(t^*))\}$
  - 23: **end for**
  - 24: Return  $\mathcal{R}$
-

$p(s^j|h^j; t^r) = \mathcal{N}(s^j; \mu^j, \Sigma^j)$ , their distance is given by [4]

$$W_2(P_i, P_j) = \left\| \mu^i - \mu^j \right\|^2 + \text{tr}[\Sigma^i] + \text{tr}[\Sigma^j] - 2\text{tr}\left[\left((\Sigma^i)^{1/2}\Sigma^j(\Sigma^i)^{1/2}\right)^{1/2}\right]^{1/2} \quad (21)$$

where  $\text{tr}$  denotes matrix trace.

This motivates the use of 2-Wasserstein distance as the decision statistics in Algorithm 1, together with the individual trajectory forecasts detailed in Section IV. The resulting computational procedure is given in Algorithm 2. Here,  $T$  is selected as a time grid over a selected interval. Note that, the use of individual forecasts as opposed to joint conditionals reduce the  $\mathcal{O}(N^2)$  complexity of finding the prediction distributions to  $\mathcal{O}(N)$ .

For each pair of trajectories, the forecast densities for the time instance  $t^r$  are found using the results outlined in Section IV. Then, the 2-Wasserstein distances of these densities are found using (21). This quantity is then tested against a threshold  $\gamma$ . If any of the distances is below or equal to the threshold, a rendezvous is declared for time  $t^r$ , and, at the centroid of the expected vessel locations.

It is instructive to compare  $(W_2(P_i, P_j))^2$  with the expectation of the squared distance when  $\mathbf{s}_{t^r}^i$  and  $\mathbf{s}_{t^r}^j$  are assumed to be completely independent and hence no (future) interactions are taken into account. For the case, the expectation of concern can easily be found as

$$E_{P^i \times P^j}\{\|\mathbf{d}_{t^r}^{i,j}\|^2\} = \|\mu^i - \mu^j\|^2 + \text{tr}(\Sigma^i) + \text{tr}(\Sigma^j). \quad (22)$$

Note that the square root of this expression upper bounds  $W_2(P_i, P_j)$  in (21), and consequently, the expected distance  $E\{\|\mathbf{d}_{t^r}^{i,j}\|\}$ . The matrix trace with the negative sign in (21) indicates that this quantity is a much looser bound compared to  $W_2(P_i, P_j)$ . Therefore, if we replace the decision statistics in Algorithm 2 with the square root of the expectation in (22), this would result with an undesirable increase in the false alarm rate. This point highlights the utility of using  $W_2(P_i, P_j)$ .

## VI. EXAMPLE

In this section we demonstrate Algorithm 2 in a simulation scenario. Fig. 1(a) illustrates 6 vessels following trajectories generated using OU processes (see Section IV) with

$$\mathbf{\Gamma} = \begin{bmatrix} 1.0e-2 & 0 \\ 0 & 1.0e-2 \end{bmatrix}, \mathbf{H} = \begin{bmatrix} 0.3e-2 & 0 \\ 0 & 1.0e-2 \end{bmatrix},$$

and sampling them at  $t = 0, 300, 600, \dots, 0.597e+5s$  over an interval of approximately 16 hours. The  $\mathbf{v}$  parameter is selected so that half of the vessels move towards East and the other half move towards North with an expected speed of  $|\mathbf{v}| = 10 \text{ m s}^{-1}$ . The initial positions of the objects are selected from two clusters as seen in Fig. 1 with slight in-cluster variation.

Vessel number 3 and 6 engage 995 minutes after initiation. The  $N(N-1)/2$  possible engagement events are depicted in

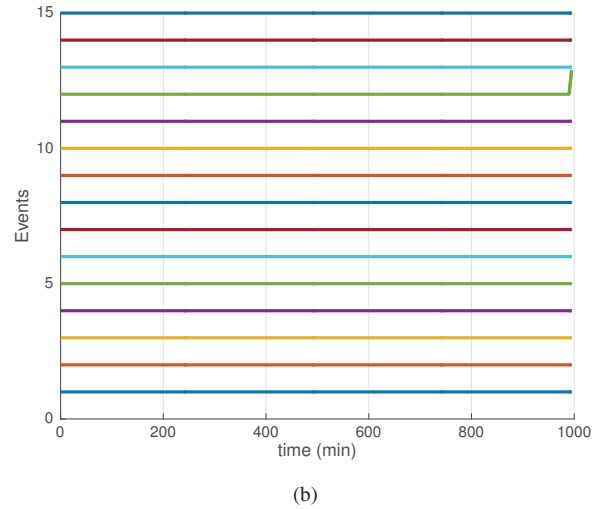
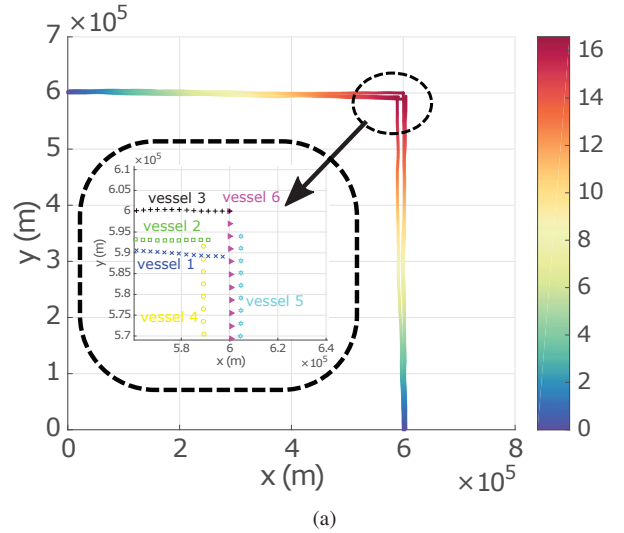


Fig. 1. Example scenario: (a) 5 objects following a OU trajectory with objects between  $t = 0 - 0.597e+5s$  (color code given in the colorbar in hours). (b) Event map for the  $N(N-1)/2$  possible rendezvous events versus time: Event number 12 encoding the rendezvous of vessel 3 and 6 at the end of the 16-hour period.

Fig. 1(b) in which event 12 indicates this rendezvous and takes a true value at the end of the 16-hour period.

We use Algorithm 2 by varying the current time from 745 to 945 minutes after the trajectories initiate. We focus on the part of the prediction interval  $T$  that forms a 20 minutes long window centered at the rendezvous event time stamp. The trajectory forecasting in line 7 is based on the OU modelling approach detailed in Section IV. Fig. 2(a) illustrates trajectory forecasts 925 minutes after the initiation. The value of the 2-Wasserstein distance decision variable for vessels 3 and 6 (possible engagement number 12) at this time instant is given in Fig. 2(b) in comparison with the expectation under independence assumption given in (22) (see Section V). The  $x$ -axis here is the prediction window  $T$  and the  $y$ -axis is the value of the decision variable corresponding to the expected

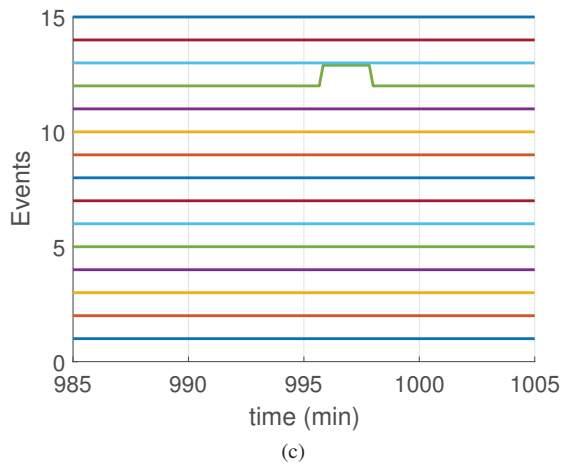
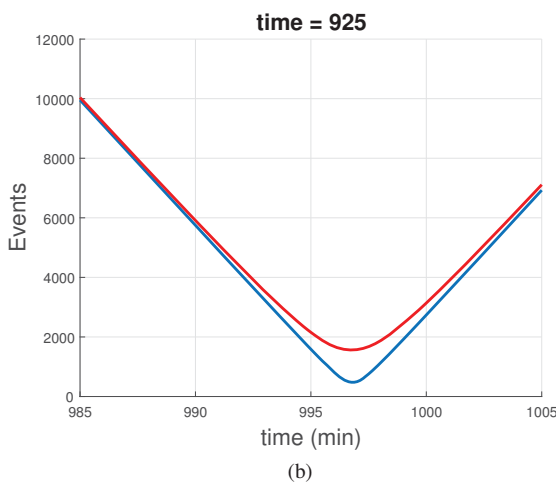
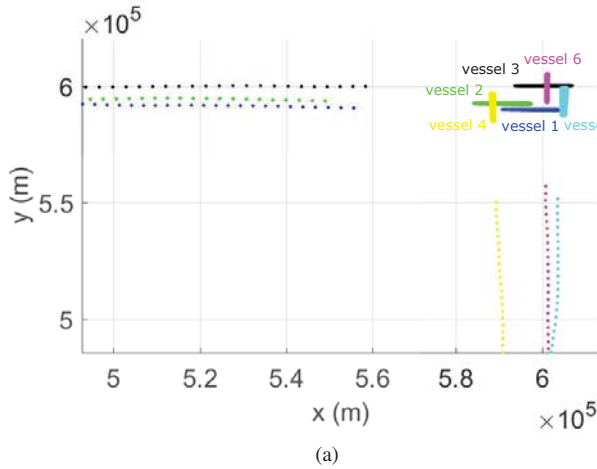


Fig. 2. Illustration of the algorithmic procedure: (a) Trajectory forecasts depicted as overlaid uncertainty ellipses of the Gaussians predicted for the time instants in a 20 minutes window around the rendezvous time each of which are found by using the up to date AIS data (dotted lines) 925 minutes after initiation. (b) The 2-Wasserstein distance decision variable versus prediction time (blue line) in comparison with the independent distance baseline (red line) at the same time instant. (c) Estimated rendezvous by the algorithm.

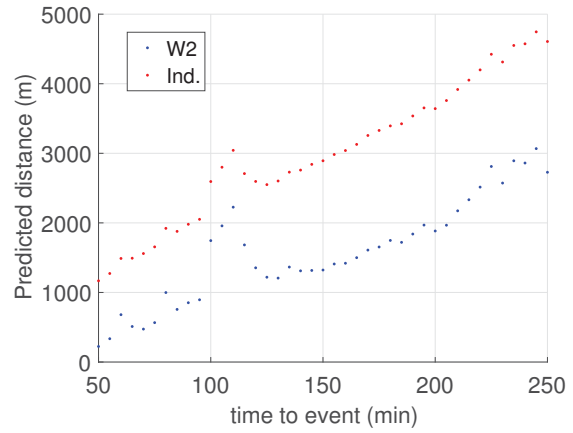


Fig. 3. The 2-Wasserstein distance versus the time difference between the prediction time and the rendezvous time. The dots are minimum values achieved within  $T$ . For comparison, values of the independent distance are provided (red dotted line).

proximity of vessels 3 and 6. The decision threshold is selected as  $\gamma = 500\text{m}$ . Note that the 2-Wasserstein distance indicates high confidancy for the engagement 50 minutes prior to the event, whereas independent distance would not be able to predict the event unless a very high threshold  $\gamma$  is selected. For a threshold of  $\gamma = 500$ , Fig. 2(c) represents the estimated rendezvous output from the algorithm.

In order to compare the quality of the decision variables, Fig. 3 gives the minimum 2-Wasserstein distance in  $T$  versus the time difference between the instant prediction is made and the rendezvous time. Here, a good predictor would take smaller values for large time difference. In this example, the 2-Wasserstein distance proves as an extremely useful metric and starts indicating very small proximity for the vessels more than 100 minutes before the event, whereas the independent distance fails to predict a distance smaller than 1000m even 50 minutes before the rendezvous.

## VII. CONCLUSIONS AND FUTURE WORK

In this article, we have considered the prediction of rendezvous from trajectory data. We proposed an algorithm which uses OU stochastic process models for forecasting trajectories and the 2-Wasserstein distance of distributions for deciding on a rendezvous hypothesis. The proposed temporal search is computationally efficient and takes into account a certain extent of future interactions which leads to a better prediction performance compared to a decision statistic that assumes independence of trajectories.

Knowledge discovery in trajectory data has become increasingly useful for maritime situation awareness. The high volume of the AIS data underpinning these applications suggest that the algorithm design should carefully take into account the trade-off between computational efficiency and accuracy. Future work involves consideration of alternative algorithms with different performance trade-offs and comparison of their efficacy on real data.

## REFERENCES

- [1] G. Pallotta, M. Vespe, and K. Bryan, "Vessel pattern knowledge discovery from ais data: A framework for anomaly detection and route prediction," *Entropy*, vol. 15, no. 6, pp. 2218–2245, 2013. [Online]. Available: <http://www.mdpi.com/1099-4300/15/6/2218>
- [2] C. Villani, *Optimal Transport: Old and New*, ser. Grundlehren der mathematischen Wissenschaften. Springer Berlin Heidelberg, 2008. [Online]. Available: [https://books.google.it/books?id=hV8o5R7\\_5tkC](https://books.google.it/books?id=hV8o5R7_5tkC)
- [3] L. M. Millefiori, P. Braca, K. Bryan, and P. Willett, "Modeling vessel kinematics using a stochastic mean-reverting process for long-term prediction," *IEEE Transactions on Aerospace and Electronic Systems*, vol. 52, no. 5, pp. 2313–2330, October 2016.
- [4] C. R. Givens and R. M. Shortt, "A class of wasserstein metrics for probability distributions." *Michigan Math. J.*, vol. 31, no. 2, pp. 231–240, 1984. [Online]. Available: <https://doi.org/10.1307/mmj/1029003026>
- [5] B. Ristic, B. L. Scala, M. Morelande, and N. Gordon, "Statistical analysis of motion patterns in ais data: Anomaly detection and motion prediction," in *2008 11th International Conference on Information Fusion*, June 2008, pp. 1–7.
- [6] P. Coscia, P. Braca, L. M. Millefiori, F. A. N. Palmieri, and P. Willett, "Multiple ornstein-uhlenbeck processes for maritime traffic graph representation," *IEEE Transactions on Aerospace and Electronic Systems*, vol. PP, no. 99, pp. 1–1, 2018.
- [7] B. I. Ahmad, J. K. Murphy, P. M. Langdon, and S. J. Godsill, "Bayesian intent prediction in object tracking using bridging distributions," *IEEE Transactions on Cybernetics*, vol. 48, no. 1, pp. 215–227, Jan 2018.
- [8] J. Murphy, E. Ozkan, P. Bunch, and S. J. Godsill, "Sparse structure inference for group and network tracking," in *2016 19th International Conference on Information Fusion (FUSION)*, July 2016, pp. 1208–1214.
- [9] L. Breiman, *Probability*, ser. Classics in Applied Mathematics. Society for Industrial and Applied Mathematics (SIAM, 3600 Market Street, Floor 6, Philadelphia, PA 19104), 1968.
- [10] B. Oksendal, *Stochastic Differential Equations: An Introduction with Applications*, ser. Universitext. Springer Berlin Heidelberg, 2013.
- [11] B. Carlin and T. Louis, *Bayes and Empirical Bayes Methods for Data Analysis, Second Edition*, ser. Chapman & Hall/CRC Texts in Statistical Science. Taylor & Francis, 2010.

# Document Data Sheet

<i>Security Classification</i>		<i>Project No.</i>
<i>Document Serial No.</i> CMRE-PR-2019-035	<i>Date of Issue</i> May 2019	<i>Total Pages</i> 7 pp.
<i>Author(s)</i> Murat Uney, Leonardo M. Millefiori, Paolo Braca		
<i>Title</i> Prediction of rendezvous in maritime situational awareness		
<i>Abstract</i> <p>In this work, we consider the problem of algorithmically predicting rendezvous among vessels based on their trajectory forecasts in a maritime environment. The problem is treated as hypothesis testing on the expected value of the distance between trajectories. We relate this quantity to the first and second degree Wasserstein distances between trajectory forecast distributions. These distributions are obtained using integrated Ornstein-Uhlenbeck process models with the trajectory measurements collected so far. Building upon these results, we propose an algorithm which traverses the trajectories observed so far for detecting rendezvous over a rolling time horizon. We demonstrate the efficacy of the proposed algorithm using simulations.</p>		
<i>Keywords</i> Predictive models, knowledge discovery, mean reverting process, Integrated Ornstein-Uhlenbeck process, Wasserstein distance, situation awareness		
<i>Issuing Organization</i> NATO Science and Technology Organization Centre for Maritime Research and Experimentation Viale San Bartolomeo 400, 19126 La Spezia, Italy  [From N. America: STO CMRE Unit 31318, Box 19, APO AE 09613-1318]		Tel: +39 0187 527 361 Fax: +39 0187 527 700  E-mail: <a href="mailto:library@cmre.nato.int">library@cmre.nato.int</a>